BRNO UNIVERSITY OF TECHNOLOGY

FACULTY OF MECHANICAL ENGINEERING

INSTITUTE OF PHYSICAL ENGINEERING

**Physics, chemistry and other aspects of one-dimensional
nanostructures' growth and analysis**

Habilitation thesis

Ing. Miroslav Kolíbal, Ph.D.   Brno 2016

Table of Contents

1. Introduction

Nanostructured materials are nowadays intensively studied because they offer improved and new functionalities over their bulk counterparts. As the number of spatial dimensions shrinks, materials exhibit new properties, unseen in bulk. A textbook example is the change in density of electronic states $D(E)$. While in three dimensions it is represented by a smooth parabola, it changes to a staircase when electrons are confined only to two dimensions (with graphene being the most attractive example of such a system). If we continue to decrease the dimensionality, we end up with zero-dimensional nanostructures, usually called quantum dots. Here, the density of states becomes a set of delta-functions and the quantum dot behaves essentially as an artificial atom. But it is not just the electrical properties that do change if a material is being simultaneously reshaped and scaled down. It is also their geometry which makes these structures appealing to use as building blocks for future devices with reduced dimensions.

This thesis deals with one-dimensional nanostructures, which are natural candidates for e.g. nanoscale circuitry, electrodes etc. One of the most exciting property of these structures is the ability to accommodate stress. That is why an increasing number of papers are dealing with nanowire (NW) electrodes in lithium-ion batteries, where the biggest problem is a crack formation upon lithiation. Significant improvement was made by the use of nanowires, which can bend and elongate during lithiation without cracking, thus lowering battery deterioration with prolonged use. While the research of nanostructured electrodes in batteries is performed on a laboratory level, nanowire-based transistors are already implemented in Intel's 22 nm technology. Here, the nanowire acts as a channel for charge carriers and its usage outperforms previous planar field-effect-transistor (FET) technology. Unlike in planar FET, where the current flowing through the channel is controlled by a gate electrode placed on top, the gate can be wrapped all-around the nanowire channel, thus increasing electrostatic control over the current flow. Consequently, the gate voltage can be significantly decreased, lowering the power consumption of the whole device. On top of that, nanowire geometry allows implementation of III-V materials as transistor channels, a long-awaited milestone that could keep the microelectronics industry on the road established by Intel's Gordon Moore in 1965.

For the fabrication of nanowire-based devices the knowledge of the NW growth mechanism is of vital importance. The research on nanowire growth is flourishing (conference on nanowire growth, NGW, is held every year since 2006) and diverse. Within this thesis, some of the mechanisms behind the one-dimensional growth of semiconductors with emphasis on selected physics and chemistry, which are of interest for the general readership, will be described. In particular, the focus will be on different collector materials than gold, including alloyed nanoparticles. Later on, several dedicated experiments will be described in greater detail, demonstrating the ongoing research in our laboratory. The text is not intended to represent a comprehensive review of the state-of-the-art in the field; instead, the reader is often referred to articles of high significance, cited throughout the text.

2. Physics and chemistry of one-dimensional growth

In general, nanowire growth from a gas phase has been rationalized by several mechanisms, including growth anisotropy due to stress [1], distinct surface free energies of different facets [2,3], differences between sticking coefficients on these facets [4], or growth rate acceleration in one dimension along a dislocation propagation direction, giving rise to complex nanowire architectures [5]. The most investigated growth technique uses metal seeds to induce one-dimensional growth (typically known as metal-catalyzed growth), and each specific growth mode is denoted by the material pathway that gives rise to growth. For example, in vapor-liquid-solid growth (VLS) [6] the metallic droplet acts as a catalyst for local decomposition of gaseous precursor molecules or as a collector of diffusing adatoms; nucleation is preferred at the solid/liquid interface between the liquid droplet and the substrate [7] and the nanowire grows with the droplet on top. A significant advantage of VLS growth is the possibility to precisely place nanowires onto a wide range of substrates [8]. VLS growth is thus by far the most popular technique for semiconductor nanowire growth today.

2.1 Vapor-liquid-solid growth and collector engineering

As mentioned above, the abbreviation VLS refers to the pathway of atoms during the growth process. The growth material is supported to the metal–coated sample from the gas-phase (Chemical Vapor Deposition, CVD) or as an atomic vapor (Physical Vapor Deposition, PVD). In former case, the molecules are decomposed preferentially on the metal nanoparticles and, hence, these are called *catalyst* (in a sense that the activation energy for precursor molecule decomposition is lower compared to the substrate material). The atoms of the semiconductor are then dissolved in the catalyst. In the latter case the metal particle has different role – it *collects* the deposited adatoms which diffuse across the substrate. Hence, the term collector is used in the following. Further steps are similar irrespective of the material supply. The atoms are dissolved in the metal particle, which sooner or later reaches the eutectic composition (concentration c_{eq}, see phase diagram in Fig. 1). If the material supply continues, the system is driven out of equilibrium as the nanoparticle is becoming rich with the semiconductor material. The only possibility for the droplet to reduce the semiconductor concentration is via nucleation of a solid semiconductor material. The nucleation probability increases with increasing concentration of a semiconductor material inside the droplet (the ratio c/c_{eq} is usually called supersaturation, S). The nucleation usually occurs at a triple phase boundary (where solid, liquid and vapor phases meet, see section 2.3) and after a stable nucleus is formed it rapidly grows in two dimensions until the full monolayer is completed. The collector is depleted of semiconductor material and for another monolayer to grow the critical supersaturation is to be reached again. Since the material is solidified below the collector *only*, the nanowires grow with it on top, having roughly the same diameter. Within this thesis, we will focus particularly on germanium nanowires, which are of interest in our group. Most of the conclusions can be applied also to silicon nanowires, with differences specifically highlighted in the text. The growth of multicomponent nanowires (e.g. III-V semiconductors) is not discussed here in detail, as it is out of the scope of this thesis. Nevertheless, the Commented paper 4 deals with SiO_x nanowire growth, and the reader can get at least a flavor of the multicomponent systems growth.
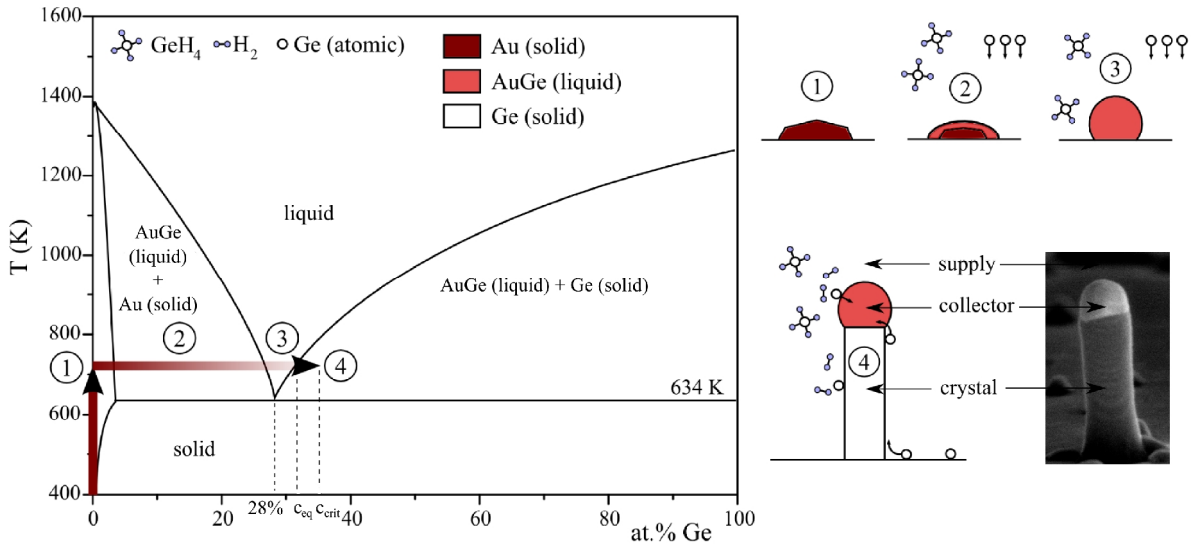
Fig. 1: *Left: Au-Ge phase diagram (after [9]), with typical reaction pathway indicated by big arrows. After heating to desired temperature (1), a solid gold nanoparticle collects germanium atoms and, potentially, gets liquid after reaching the liquidus line (2 and 3). If Ge atoms supply is not stopped, their concentration within a droplet increases, together with the nucleation probability (4). Note that during initial phases 2 and 3, the droplet can potentially consume material from a substrate and, thus, no external supply is needed to form the eutectic droplet. The phase diagram shown here is for bulk, but potentially large deviations were reported for small size droplets [10]. Right: Schematic illustration of main processes during VLS nanowire growth above eutectic temperature. Solid gold (1) collects the germanium atoms. First a liquid surface layer is formed (2) [11] followed by formation of an eutectic liquid droplet (3). Continuous supply of Ge atoms from gaseous precursor (germane molecules which decompose on the collector surface) or atomic vapor (Ge atoms diffuse towards the collector and are incorporated) results in nanowire growth, with collector droplet on top. The image taken by scanning electron microscope shows germanium nanowire (120 nm diameter) with solidified Au collector droplet on top.*

The material pathway in VLS growth is ensured only if a following condition is met:

$$\mu_{s} > \mu_{c} > \mu_{k}, \qquad (1)$$

where μ_{s}, μ_{c}, μ_{k} is the chemical potential of atoms in supply, collector and crystal phase (nanowire), respectively. Note that if μ_{c} reaches its upper bound (μ_{s}) the accommodation of the material by the collector will stop and, indeed, if $\mu_{s} < \mu_{c}$ the material will desorb from the collector to vapor phase. The same applies to the other inequality, if $\mu_{c} < \mu_{k}$ the solidified material will be dissolved in the collector.

The terms supply, collector and crystal were adopted from [7] and will be used throughout this thesis instead of more common terms vapor, liquid and solid from pedagogical reasons. Also, in nanowire related literature, it is common that the chemical potential change between collector and crystal phase ($\Delta\mu_{ck}$) is denoted as supersaturation, instead of S. Note that these quantities are related via $\Delta\mu_{ck} = kT \ln S$, and here we will distinguish between the two.

While we will focus on some other aspects of this growth mode later, let's discuss what the appropriate material choice is for the collector. By far the most

6

utilized metal for the nanowire growth is gold. Its biggest advantage is the chemical stability and low-temperature eutectic formation with materials of interest (group IV, III-Vs and even ternary compounds or oxides). However, for applications of nanowires in semiconductor industry gold could be detrimental as it forms electronic mid-gap states within the bandgap of many semiconductor materials. Therefore, the presence of gold atoms in the growth process unavoidably raises questions on their incorporation into the nanowire [12-15], which may be detrimental for nanowire-based device operation. Another disadvantage of gold is relatively high group IV element content at eutectic concentration, which severely limits the use of similar collector materials (Al, Ag) for axial heterostucture growth. When the supply is changed, the collector first depletes of previous material, depositing a mixture of both materials, and, subsequently, deposits the new one. This is called the reservoir effect and inevitably results in diffuse interface instead of a sharp one. It seems that elements exhibiting very low eutectic concentration with materials of interest are an ideal choice, as the reservoir effect is minimized and the growth temperature significantly lower. Liquid metals (e.g. Ga, In, Sn, Sb) indeed meet these requirements (see Ga-Ge phase diagram in Fig. 2a). However, it turns out that these elements have relatively low surface free energy and thus prefer to spread across the nanowire sidewalls instead of being pinned on top of a nanowire (the so-called Nebolsin criterion [16]). Another issue could be the low solubility. The very steep liquidus line in Fig. 2a indicates relatively large energy cost required to push the system out of equilibrium concentration. This hypothesis seems to be confirmed experimentally, since the successful growth utilizing pure Ga collector was conducted using plasma-enhanced deposition only [17].

An alternative solution of this issue came with the discovery that in some cases the presence of eutectic (liquid) phase is not necessary to promote nanowire growth and the nanowires can grow utilizing solid collector [18-19], where the solubility of nanowire material is also very low. This is usually the case of materials whose phase diagram predicts several phases and usually high eutectic temperature (Cu, Mn etc.). At this point, it is interesting to summarize that collector materials can be generally classified into three groups based on their phase diagram, which was first introduced by Bootsma et al. [20] and summarized by Schmidt et al. [21].
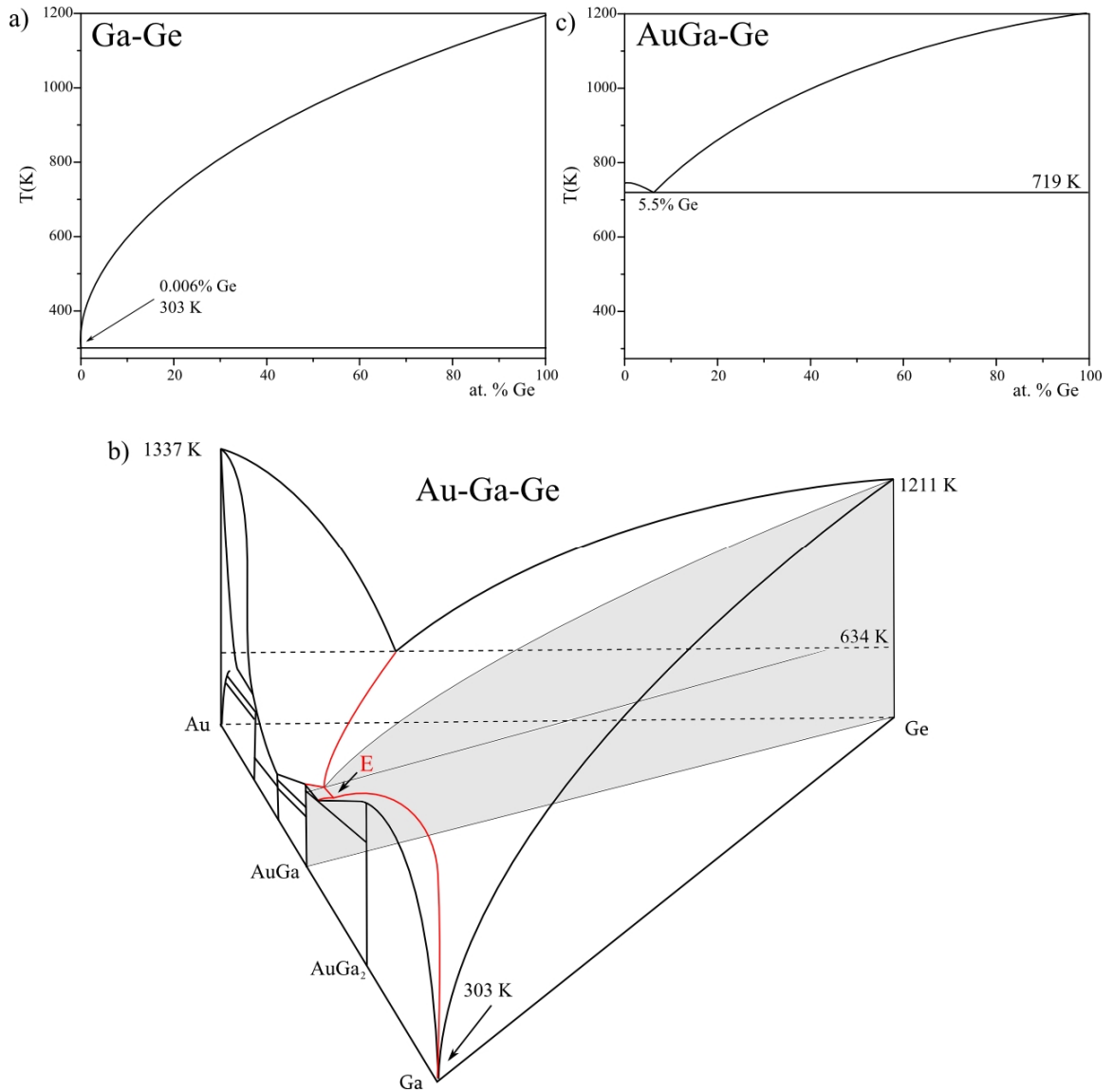
Fig. 2: a) *Ga-Ge phase diagram (after [22]), exhibiting the eutectic point at 303 K for 0.006% Ge. b) The ternary phase diagram is three-dimensional and has a shape of a triangular prism with temperature plotted on the vertical axis. The sidewalls of the prism represent three binary phase diagrams. A sketch of such a plot is shown here, with estimated liquidus line [23] in red and the ternary eutectic point marked E. It is difficult to read such a plot, hence the information is usually plotted in two dimensions by cross-sectioning the plot in different ways (being dependent on the information requested). For our purposes, it is instructive to slice the plot as indicated in the Figure (section plane marked in grey). In this case, Au-Ga ratio is fixed to 1:1 and the resulting pseudobinary phase diagram (after [23]) exhibits the eutectic point at 719 K for 5.5% Ge (c). Clearly, by varying the composition of the initial alloyed phase the eutectic point position can be tuned.*

However, the reproducibility of the growth utilizing solid collector is poor as compared to VLS, because the nanowire epitaxial relationship to the substrate is dependent on the seed particle orientation to the substrate [24]. A very promising and still relatively unexplored approach is to use alloyed collectors, where one of the components is a liquid metal. The other component is chosen to stabilize the droplet

against Nebolsin criterion and increase (or otherwise manipulate) the solubility of nanowire material (see Fig. 2b,c). The tunable alloy composition allows optimization of growth conditions, not to mention that it affects also other physical properties of the resulting one-dimensional structure (orientation, faceting, defect and polytype formation to name just a few).

2.2 Gibbs-Thompson effect

The collector is a central to VLS growth. It is fundamentally appealing to grow nanowires with very small diameters, but if that goal is to be approached via VLS growth mechanism, one faces a severe thermodynamic restriction posed on the collector diameter – the so-called Gibbs-Thompson effect, which will be introduced in this section.

The derivation will start with definition of the total differential of Gibbs free energy of N atoms within a droplet having volume V:

$$dG = Vdp - SdT + \mu_{\infty}dN + \gamma\,dA, \tag{2}$$

where p is the pressure, μ_{∞} is the chemical potential (assuming droplet of infinite size), S is the entropy, T is the temperature and γ is the surface free energy. The first two terms vanish as the pressure and temperature are held constant, and the expression simplifies to

$$dG = \mu_{\infty}dN + \gamma\,dA.$$

Let's consider the droplet to be a hemisphere having a diameter r, then the infinitesimal change in droplet surface dA and volume dV upon addition of dN atoms (with atomic volume Ω) is

$$dA = 8\pi r dr,\ dV = 4\pi r^2 dr = \Omega\,dN.$$

Combining these expressions together we get

$$dA = \frac{2\Omega}{r}\,dN,$$

and, substituting to eq. 2 (assuming a constant pressure and temperature):

$$dG = \left(\mu_{\infty} + \frac{2\gamma\Omega}{r} \right)dN.$$

Recalling that $\mu = \partial G/\partial N$ we finally arrive at a well-known expression for the chemical potential [21],

$$\mu = \mu_{\infty} + \frac{2\gamma\Omega}{r}\,. \tag{3}$$

Apparently, the dependence of chemical potential on collector diameter implicates the existence of critical diameter, below which the nanowires cease to grow [25, 26] because the supersaturation necessary for nucleation would not be reached. This has indeed been observed experimentally [26] and the Gibbs-Thompson effect is responsible for the characteristic decrease in nanowire growth rate with decreasing nanowire diameter [27].

2.3 Preferential nucleation

It is also interesting to discuss why the nuclei form below the collector, and not anywhere else. There are several possibilities, as shown in Fig. 3. Although formation of nucleus (ii) seems unfeasible, according to argumentation presented so far it's the most probable case! Note that according to eq. 1 the chemical potential difference between vapor and solid phase is larger than liquid and solid phase; the supersaturation in the liquid with respect to solid is always smaller than that in the vapor. The one-dimensional growth cannot be therefore explained using inequality of chemical potentials only.
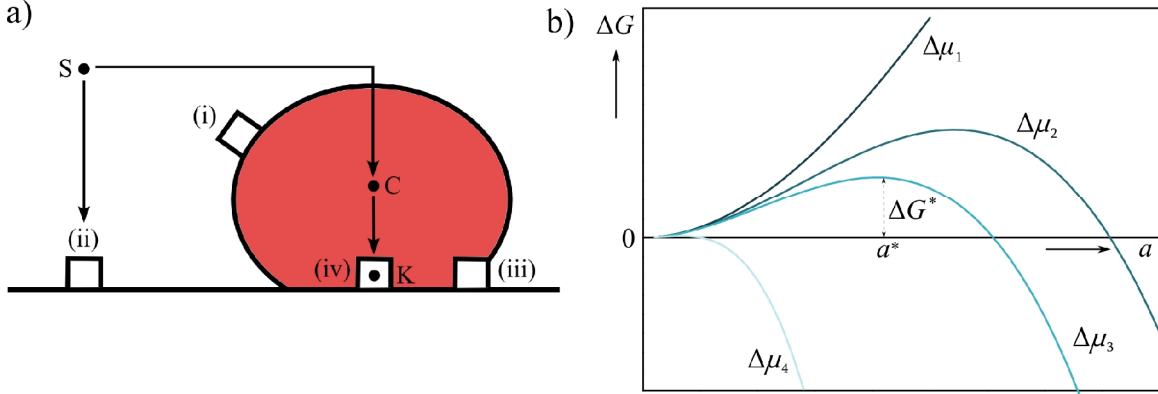
Fig. 3: a) *Schematic showing nucleation at different interfaces from a supply (S) via collector (C) at the crystal (K). Heterogeneous nucleation (i), homogeneous nucleation from a supply phase (ii), from collector at the triple phase boundary (iii) and at the collector-crystal interface (iv). b) Gibbs free energy change dependence on characteristic size for different supersaturations ($\Delta\mu_1 < \Delta\mu_2 < \Delta\mu_3 < \Delta\mu_4$). For one of the curves ($\Delta\mu_3$), also critical nucleus size a^* and nucleation barrier ΔG^* are shown.*

The driving force for the nucleation of a new phase (solid nucleus in our case) from an old one is a positive free energy difference between the old phase and a new crystalline phase plus the final old phase [28]. Specifically, for nucleus (i) in Fig. 3a with cubic shape with characteristic size a, it can be quantified as

$$\Delta G = \Delta G_b + \Delta G_s = -\frac{a^3}{\Omega}\Delta\mu_{ck} + \left(5a^2\gamma_{cs} + a^2\gamma_{ck}\right), \qquad (4)$$

where ΔG_b and ΔG_s are bulk and surface related free energy change, respectively, and the subscripts "cs" and "ck" refer to the collector-supply and collector-crystal interface, respectively. Plotting ΔG versus a for different supersaturations (Fig. 3b) results in a well-known dependence, exhibiting a maximum in ΔG for certain a^* (critical nucleus size). The maximum value ΔG^* is called nucleation barrier and enters the expression for a nucleation rate in an exponential term $\exp(-\Delta G^*/kT)$. We will not provide more details here, as the reader can find more sophisticated description of the classical nucleation theory elsewhere [29], but summarize the conclusions which can be deduced from Fig. 3b. If the nucleus size a is smaller than the critical nucleus size a^*, its growth is not possible as the free energy of the system would increase. On the contrary, nuclei larger than a^* can grow. Clearly, the droplet supersaturation (which enters the bulk related term in eq. 4 by $\Delta\mu_{ck} = kT \ln S$) can significantly alter a^* (and, hence, nucleation barrier). If the supersaturation is very high, the critical nucleus size becomes smaller than the growth unit and the nucleation barrier vanishes. Then the

old phase becomes unstable and spontaneous nucleation occurs (see Commented paper 4, mentioning this effect).

The nucleation barrier is affected also by the surface term in eq. 4. It differs for different nuclei positions (Fig. 3a) and, thus, leads to an understanding of which interfaces are preferred for nucleation. E.g. it is more likely that nucleus (ii) will be formed instead of nucleus (i), because the surface-related Gibbs free energy increase is smaller for homogeneous nucleation compared to heterogeneous case. However, in a three phase system, which is the case here, the degree of supersaturation can potentially outweigh surface related term. It turns out that it is often the case for nucleus (iii), located at the triple phase boundary (TPB). It has been hypothesized that the local supersaturation is highest at TPB, because it is in direct contact with the supply [7] and, additionally, this interface is rough and faceted [30] (which decreases the nucleation barrier). One-dimensional growth therefore results from preferential nucleation at a specific interface, while nucleation on other interfaces is suppressed.

3. Role of in-situ microscopies

Similar to other research fields in experimental physics, the biggest breakthroughs in our understanding of the nanowire growth aspects were achieved using unique instrumentation, in this particular case it is in-situ electron microscopy. In-situ microscopic techniques are very attractive as they allow visualization of the process in question with superior spatial and time resolution [31]. The most valuable experiments were carried out in the group of Frances Ross at IBM Yorktown Heights (eutectic formation [32], initial nucleation events [33], layer-by-layer growth below the droplet [34], nanofacet oscillation at the TPL [30], subeutectic growth of Ge NWs [11]). Transmission electron microscopy (TEM) offers unprecedented spatial resolution and fast image acquisition. However, one has to bear in mind that the image is a planar projection – to get the three-dimensional information, complicated procedures are required. Additionally, the sample preparation is troublesome – usually, the nanowires are pre-grown in conventional CVD reactor and after the growth a small piece of substrate is cut out of the sample for subsequent growth in TEM. These disadvantages are circumvented if scanning electron microscope (SEM) is to be used. Although the superior resolution of TEM is lost, SEM allows characterization of the sample in three-dimensions without complicated sample preparation procedures. With this in mind, we successfully attempted to transfer the previously developed growth procedure for germanium nanowires into SEM for the first time. We have focused onto the collector droplet, which is central to the VLS process, and successfully related the droplet behavior to the observed nanowire morphologies (Commented papers 1-3). While the germanium nanowire growth was achieved utilizing PVD in high vacuum (1×10^{-4} Pa), real-time observation of CVD-like process is even more challenging. To achieve this goal, we have built an environmental reaction cell inside SEM, which allows SEM imaging at high gas pressures, and studied the growth of silica nanowires using gallium collector (Commented paper 4).

4. Commented paper 1, dealing with initial stage of the germanium nanowire growth and growth direction[1]

From the post-growth microscopic observations, it is known that metal droplet shape changes between the very beginning of growth and the stable nanowire growth – the droplet contact angle with the substrate (and nanowire, subsequently) significantly increases (this is schematically depicted in Fig. 1), and nanowires exhibit a tapered pedestal. The first theoretical treatment of the problem was given by Schmidt et al. [35], showing excellent agreement with experiment. However, the model did not account for faceting of semiconductor surfaces, which is often observed at elevated temperatures. The simulations of nanowire growth including formation of new facets were presented in two papers by Schwarz and Tersoff [36, 37]. This model predicted the formation of tapered faceted pedestal, as well as nanowire growth orientation dependence on the deposition rate.

We demonstrated the formation of different facets experimentally by microscopic observation of initial growth interface formation on Ge(100) substrate (Fig. 4a), which has a pyramidal shape. However, the droplet cannot wet all the four pyramid sidewalls, and it slides across the two of them, finally wetting the remaining two only. This observation explains the formation of the V-shaped interface, which is the inherent property of the <110>-oriented nanowires [38]. This finding was also the first observation of the droplet instability, studied in detail in Commented paper 2. Similar experiments on different substrates (Fig. 4b), performed after the paper was published, confirmed the conclusions made earlier.
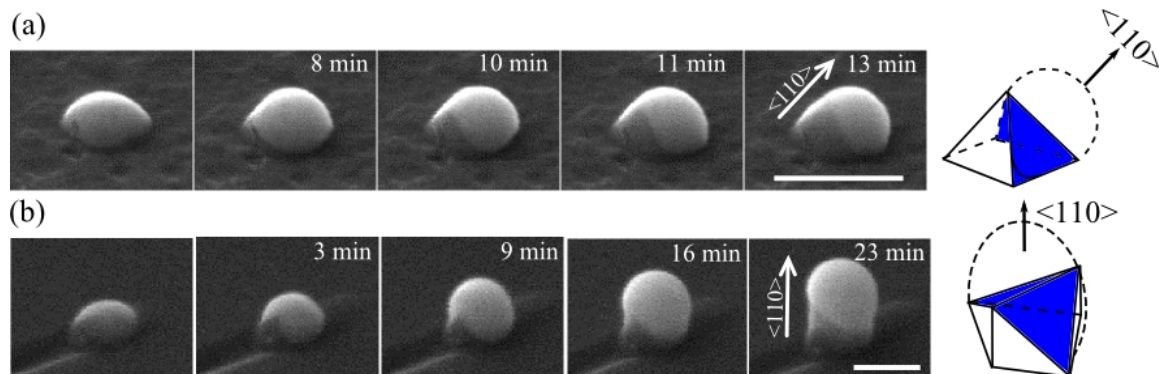
Fig. 4: *The formation of the V-shaped growth interface, possessed by nanowires growing in <110> direction from different substrates. a) An image sequence captured using scanning electron microscope at elevated temperature (400 °C) during Ge evaporation (evaporation rate 3 Å/min) onto Ge(100) substrate covered with Au nanoparticles (bright droplet in the middle of the image). Initially, a germanium island having a pyramidal shape with {111}-oriented sidewalls evolves. However, the droplet dewetts two of them (visible 10 minutes after observation start) and finally pins to the edges of the remaining two, thus forming the V-shaped interface made of two inclined {111} planes (marked blue in the schematic to the right). Similar experiment, viewed from different angle, is shown in Fig.2 in the Commented paper 1. b) Another experiment performed at higher evaporation rate (12 Å/min) on Ge(110) substrate. Again, the V-shaped interface is formed and in this case the nanowire*

---

[1] Kolíbal, M.; Vystavěl, T.; Novák, L.; Mach, J.; Šikola, T. *In-situ observation of <110> oriented Ge nanowire growth and associated collector droplet behavior*. Appl. Phys. Lett. 2011, 99, 143113.

grows perpendicular to the substrate. Note that if such a relatively high evaporation rate is used, also <111>-oriented nanowires grow (see commented paper 2). Scale bars, 200 nm. The images are tilted by 52° to the surface normal.

The increased interest of scientific community in controlling the nanowire growth orientation is driven by demands of semiconductor industry. For designing wrap-all-around-gate transistors, it is necessary to grow nanowires perpendicular to the substrate, which is nowadays almost exclusively Si(100) due to its superior oxide/surface interface. Unfortunately, nanowires grow mostly in <111> and <110> directions. The latter growth direction prevails for nanowires with diameters smaller than 20 nm, which has been demonstrated experimentally [26] and explained theoretically [39]. However, germanium nanowires grown by PVD are exceptional from this rule – independently on diameter, they grow in <110> direction. While in our latest work (to be published) we demonstrate that the difference is caused by sidewall chemistry (hydrogen-termination of sidewalls in case of CVD), here we have verified the model of Schwarz and Tersoff [37] predicting that by increasing the deposition rate (and, hence, the nanowire growth rate) the nanowire growth direction changes from <110> to <111> due to different facet growth velocities. Additionally, we provide an alternative explanation of the <111> to <110> transition for small nanowires grown by CVD. If the Gibbs-Thompson effect (eq. 3) is accounted for in eq. 1, we get

$$\mu_{\text{s}} > \mu_{\text{c},\infty} + \frac{2\gamma\Omega}{r} > \mu_{\text{k.}}$$

The chemical potential difference between the source and the collector governs the incorporation rate of the atoms from the supply into the droplet, which drops significantly when the droplet dimensions get smaller (where the contribution of the Gibbs-Thompson effect gets significant). This results in slower nanowire growth (in case of incorporation-limited regime, which is usually the case [40]) and, hence, in change of the nanowire growth direction. It is interesting to note that even if one reaches the goal to grow the nanowires with certain crystallographic orientation, the situation is far more complicated as there are usually more members of each family of crystallographic orientations (see Fig. 5) and, additionally, the formation of twin defects could cause nanowires to grow in directions with no epitaxial relationship to the substrate [41]. Another issue is thus to force the nanowires to grow at one specific orientation, which is still very active field of research.
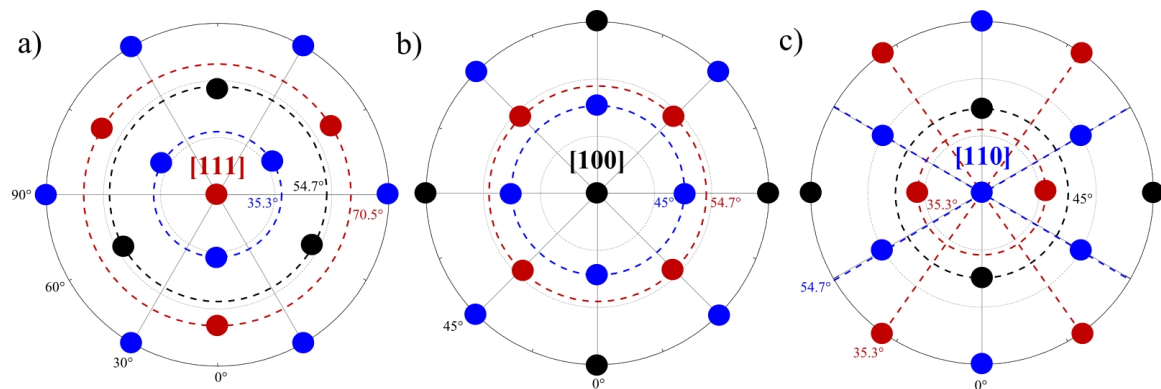
Fig. 5: *Stereographic projections with respect to a) [111], b) [100] and c) [110] orientations. Black dots, <100> direction; red dots, <111> direction; blue dots <110> direction. Other crystallographic directions are not shown for clarity.*

Degrees on perimeter designate azimuth angles, degrees close to circles designate inclination angle with respect to the surface normal (the perimeter lies in the surface plane, i.e. the inclination angle is 90°).

5. Commented paper 2 (Nano Letters 14, 1756), dealing with droplet instability on top of a nanowire[2]

The nanowires are in an ideal case long, straight and untapered (i.e. their diameter does not change along their growth axis). This is often not the case – nanowire sidewalls are faceted (see Commented paper 3), the diameter is modulated along the axis or, most importantly, kinks (changes in the growth direction) are present. The kinking was assumed to result from the droplet motion on the top of a nanowire, where a new facet is formed and rapidly grows, while being wetted by the droplet. In the end the nanowire growth direction is changed according to this new facet orientation.

In this paper, we have intentionally grown <111>-oriented germanium nanowires using very high deposition flux (see Commented paper 1), which possess three inclined sidewall facets that are not perpendicular to the growth interface. From post-growth microscopic images it was uncertain how such a complex morphology is formed. Using real-time microscopy, we have observed that the droplet is not pinned to the topmost (111) growth interface, but periodically wets down the sidewall facets, thus allowing their growth (Fig. 6). This finding is unique as it shows that the droplet instability does not always result in kink formation. Instead, straight nanowires can grow with the droplet periodically wetting different facets on top of a nanowire.
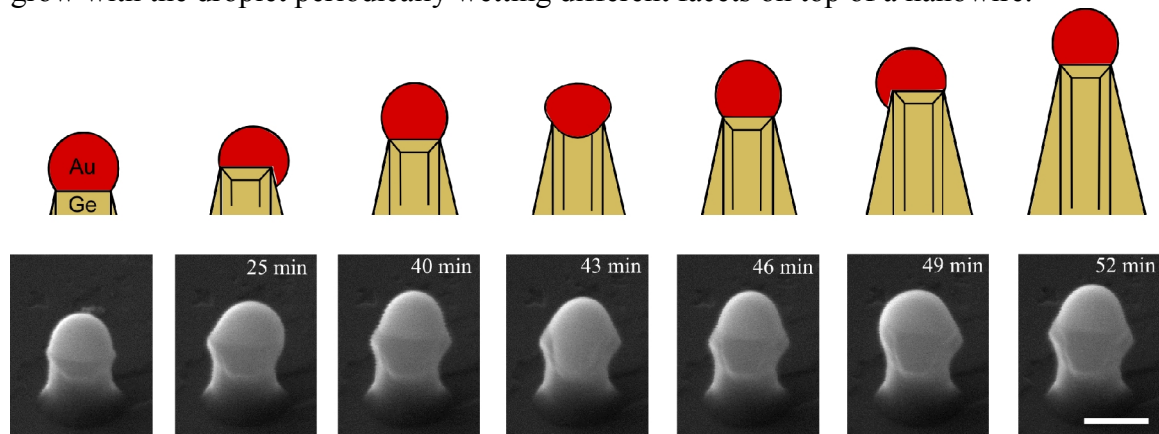
Fig. 6: *The image sequence (bottom) demonstrates the droplet motion on top of a <111>-oriented nanowire, growing at 400 °C on Ge(111) substrate. The collector (bright droplet on top of a nanowire) repeatedly wets the adjacent sidewalls, which overgrow into a hut-like shape (see the paper for details of the nanowire morphology). Despite the instability, the nanowire grows straight in the <111> direction (schematically shown on top). Scale bar, 200 nm. The images are tilted by 52° to the surface normal.*

The explanation of the droplet motion is based on a fact that there exists a certain range of contact angles where the droplet is pinned to the substrate (the so-called Gibbs inequality). Because the droplet is geometrically frustrated [42] due to non-parallel sidewall facets (that is, as the growth proceeds, the top (111) growth

---

[2] Kolíbal, M.; Vystavěl, T.; Varga, P.; Šikola, T. *Real time observation of collector droplet oscillations during growth of straight nanowires*, Nano Letters 2014, 14, 1756.

interface shrinks), the contact angle sooner or later leaves the stable range and the droplet unpins from the top facet and starts to wet also sidewall facet. The same mechanism applies for another pinning/unpinning events and the straight nanowire growth is maintained. This mechanism seems to be general, as it can explain the unusual nanowire morphologies observed in our experiments, as well as other nanowire shapes with diameter modulation.

After this paper was published, similar effect was reported by IBM group [43]. In their experiment, the droplet instability is caused by its decreasing volume, which also results in similar geometrical frustration.

6. Commented paper 3, dealing with nanowire faceting and cross-section[3]

Although not highlighted in the introductory sections, one of the main advantages of VLS growth is the superior ability to control the nanowire diameter via dimensions of the collector droplet. The nanowires are usually presented to have a cylindrical shape, with smooth sidewalls. However, semiconductor nanowires are often faceted, and the circular cross section is a rough approximation. Nanowires exhibit sidewalls with crystallographic orientations being specific for different materials and growth directions [44, 45]. Most of the nanowires growing in <111> direction possess hexagonal cross-section. There are few studies reporting other cross-sections (nanowires having four sidewalls or even triangular cross-section). It is interesting to note that nanowires can grow in <111> direction despite the fact that there exist no stable facets parallel to <111> direction. Except germanium nanowires reported in second commented paper, another example of such behavior are silicon nanowires, which exhibit sawtooth-faceted sidewalls [46], which are formed by short alternating segments with {111} and {311} orientations due to Au-induced faceting. The sidewall crystallographic orientation is important for many applications, it is e.g. crucial for sensing.

It is interesting to consider why the germanium nanowires exhibit mostly {111} oriented sidewalls. The equilibrium crystal shape of germanium was determined by Stekolnikov and Bechstedt [47], utilizing the Wulff construction with calculated surface free energies of different facets as input values. The resulting shape is shown in Fig. 7a. Interestingly, {111} facets do not seem to be dominant and, conversely, a large variety of facets with different orientations is present. There are two plausible explanations, both similar in nature. Surface free energy can change with adsorption of various species. These could be adsorbed atoms and molecules from the ambient atmosphere inside the growth chamber (e.g. [48]) or metal atoms (e.g. gold atoms from a collector), which usually induce surface reconstruction. To decide which explanation applies to the germanium faceting an additional work is needed, however, our preliminary results strongly indicate that latter mechanism is responsible for {111} facets preference (see Fig. 7b, c). Just recently, we have successfully proven this hypothesis by site-selective Auger spectroscopy (to be published).

---

[3] Kolíbal, M.; Kalousek, R.; Vystavěl, T.; Novák, L.; Šikola, T. *Controlled faceting in <110> germanium nanowire growth by switching between vapor-liquid-solid and vapor-solid-solid growth*, Appl. Phys. Lett. 2012, 100, 203102.
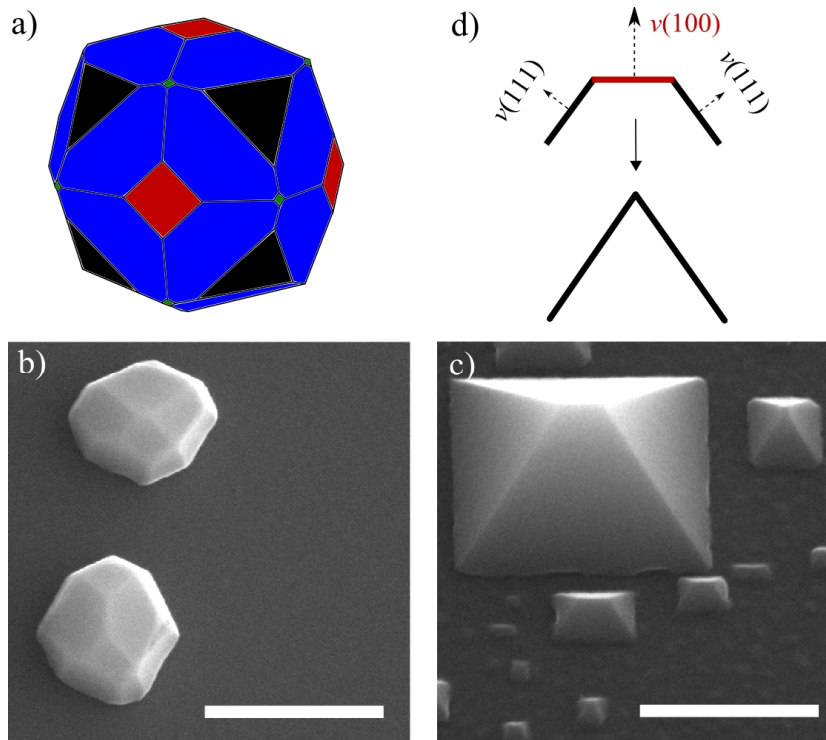
Fig. 7: *a) The equilibrium crystal shape of germanium, as calculated in [47]. The surface planes are marked as follows: {100} planes, red; {111} planes, black; {311} planes, blue; {110} planes, green. b,c) Experimentally observed crystal shapes deposited by evaporation of Ge at 600 °C onto (b) clean Ge(100) surface and (c) Ge(100) surface with submonolayer coverage of gold. Note that on gold-free substrate the islands exhibit numerous facets, similar to the theoretical prediction in a). If gold is present, {111} facets are strongly preferred, as deduced from the island geometry. Note that these island shapes are observed within temperature window of interest (400-600 °C). If substrates with different crystallographic orientation are used, the island shape changes, but the preference for {111} facets remains. Scale bars, 500 nm. The images are tilted by 60° to the surface normal. d) A schematic showing three facets (two {111} facets and one {100}) growing at different velocities as indicated by the arrows. Such a geometry represents a partial top view onto the growth interface of <110>-oriented nanowire. Clearly, as the {100} facet grows faster, it shrinks in time until it finally diminishes.*

In this commented paper, we have focused on a puzzling observation that germanium nanowires grown in <110> direction by PVD have a rhomboidal cross section (four sidewalls having {111} orientation). This is surprising, because according to simulations the droplet cannot wet the sharp corners of the nanowire top facets. Utilizing real-time in-situ electron microscopy we have shown that nanowires grow initially with hexagonal cross-section (with two additional {100} sidewall facets) and the rhomboidal cross-section is a result of an uncatalyzed overgrowth of these two facets. Moreover, we demonstrate the ability to control the cross-section by switching the droplet between liquid and solid states, thus preparing segments with different sidewalls. To explain this behavior, we have modified the model published by Froberg et al. [27] by including a collecting activity of the droplet, which decreases when the droplet solidifies. Unlike in CVD, where germanium nanowires can be grown below the eutectic temperature [49], this was not reported up to date using

PVD. It may be due to an extremely slow growth or absence of the adsorbed hydrogen [50], but more likely due to a fact that the supersaturation is not that high to prevent Au solidification, and the chemical potential of the solid collector significantly decreases. As a consequence, the driving force for atom incorporation into the collector decreases, and the diffusing adatoms could be incorporated at steps. {100}-oriented facets grow faster than {111}-oriented ones as they possess higher surface free energy. Because of mutual inclination between faceted sidewalls (Fig. 7d), {100} facets finally diminish and only four {111} sidewalls remain.

7. Commented paper 4, dealing with preferential nucleation on an oxide shell encapsulating the liquid metal collector[4]

As stated in section 2.1, the search for alternatives to gold is very active field of research. In this respect, liquid metals (metals with extremely low melting point – Ga, In, Sn) are very attractive and promising for the growth of nanowires at low temperatures and for fabrication of heterostructures due to suppressed reservoir effect. However, the low solubility of materials of interest in these metals results in severe obstacles in the growth of nanowires using VLS growth regime. To reach the supersaturation for nanowire growth and nucleation, it seems necessary to deliver the growth species as plasma-generated radicals [17]. The growth is therefore performed using alloyed collectors [51], while the studies reporting nanowire growth utilizing pure liquid metals are sparse [52]. On the contrary, numerous reports were published where the growth of oxide nanowires (mainly SiO_2) was demonstrated utilizing liquid metals [53]. Although they exploit some common properties which differ from the NWs grown by VLS, the plethora of observed morphologies was not explained. Additionally, the root-growth mode (where numerous nanowires grow from a single collector droplet, which is located at the nanowire bottom) was not fully rationalized yet.

In Commented paper 4, we have focused on a specific material system (gallium collector droplet, silicon oxide nanowires). Unlike previous nanowire growth experiments performed by other groups using conventional CVD reactors, we have employed an ultrahigh vacuum chamber with precisely controlled gas inlets, real-time scanning electron microscopy and a range of in-situ and ex-situ spectroscopic techniques. This allowed us to identify the key role of water in the nanowire growth, the material supply pathways, processes that limit the growth rate and other aspects of the nanowire growth mechanisms (e.g. movement of collector droplet during growth). We demonstrate the critical role of thin oxide layers on growth, and explain numerous contradictory results in the literature. Our experiments shed light on the origins of the root-growth mechanism, which is not fully understood despite being widely reported in the literature. We demonstrate that the native gallium oxide is preferential nucleation place (see section 2.3). The supersaturation for nucleation is lower at the collector/oxide interface compared to collector/substrate, which rationalizes the growth of nanowires with collector at the bottom. The root-growth mode reported here allows fabrication of nanowires with very small diameters (<10 nm) and thus circumvents the thermodynamic Gibbs-Thompson effect, which limits the growth of extremely small nanostructures using metal collectors (see section 2.2).

However, the initial multiple nucleation was not explained yet [54] and is still awaiting for full clarification, despite some promising attempts [55] explaining the

---

[4] Kolíbal, M.; Novák, L.; Shanley, T.; Toth, M.; Šikola, T. *Silicon oxide nanowire growth mechanisms revealed by real-time electron microscopy*. Nanoscale 2016, 8, 266.

phenomenon by spinodal decomposition (vanishing of the nucleation barrier at very high supersaturations, which results in instability of the collector phase and spontaneous multiple nucleation events, see Gibbs free energy dependence for $\Delta\mu_4$ in Fig. 3b).

8. Additional aspects of nanowire growth and analysis

Although our research is targeted primarily onto fundamental aspects of nanowire growth, it is inevitably accompanied with other topics dealing with analysis of nanowire properties and their potential utilization in future devices. The results commented in this chapter go beyond the traditional nanowire-based research as they turned out to be interesting topics on their own. Commented paper 5 deals with controlled placement of individual colloidal nanoparticles onto a semiconductor substrate, primarily aimed at possible growth of ordered nanowire arrays. Soon it became clear the developed particle positioning technique is of utmost importance for plasmonics, where the gold nanoparticle arrays are used to prepare metamaterials with various extraordinary properties [56]. Similarly, the results on dopant concentration determination presented in Commented paper 6 are widely applicable to almost any semiconductor sample and are not limited to nanowires only. The story behind Commented paper 7 is different, as we have realized just later on that the described procedure for germanium nanofabrication is of crucial importance for preparation of nanowire samples for TEM observation. The first two papers presented in this chapter were prepared in close cooperation with master and PhD students under my supervision.

8.1 Commented paper 5, dealing with assembly of gold colloidal nanoparticles into regular patterns[5]

The growth of ordered nanowire arrays (i.e. arrays consisting of regularly spaced nanowires in a repetitive pattern) is a necessary prerequisite for integration of nanowire-based devices onto current CMOS platform. The catalyst metal can be patterned by usual means of electron beam or optical lithography, including metal deposition and lift-off process. However, the best uniformity in nanowire diameters is achieved if colloidal metallic nanoparticles are used. In this case, different patterning techniques have to be employed, utilizing electrostatic interaction between the colloidal nanoparticles and the substrate, selective chemical functionalization of the surface, or modification of substrate morphology to name just a few. All these techniques require presence of a thin, usually organic layer on the substrate surface, which could be detrimental to the nanowire growth. In an attempt to avoid using such a layer we have come up with a new technique for the preparation of ordered nanoparticle arrays deposited from colloidal solution, based on ion or electron beam exposure of the bare semiconductor surface.

Semiconductor surfaces (Si, Ge, III-Vs) are usually covered by a thin native oxide layer, which determines the nature of adsorbed molecules. In case of silicon, the native oxide is in most cases terminated by hydroxyl groups (-OH). When such a surface is dipped into an aqueous solution, depending on pH of the solution the surface groups exhibit positive charge (-OH$_2^+$ at low pH), negative charge (-O$^-$ at high pH) or remain electrically neutral (at the so-called isoelectric point). Since the

[5] Kolíbal, M.; Konečný, M.; Ligmajer, F.; Škoda, D.; Vystavěl, T.; Zlámal, J.; Varga, P.; Šikola, T. *Guided Assembly of Gold Colloidal Nanoparticles on Silicon Substrates Prepatterned by Charged Particle Beams*. ACS Nano 2012, 6, 10098.

nanoparticles in colloidal solution also bear an electric charge (depending on the preparation technique), we have successfully utilized these properties to prepare ordered colloidal arrays by either removing or changing the surface terminating groups by focused ion and electron beams (see Fig. 8). The experiments shown in the paper demonstrate that the colloidal nanoparticles can adsorb either on the beam-exposed areas or pristine ones only, thus mimicking the conventional positive and negative lithography process.

Although the present paper deals exclusively with silicon, it is applicable also to other semiconductor surfaces. The utilization of an electron microscope is advantageous, especially in case that the surface chemistry of the surface of interest is unknown. By introducing different gas precursors into the microscope chamber during patterning by the particle beam the surface termination can be altered in-situ and, thus, suitable surface termination allowing the above mentioned patterning strategy can be found. Although being slow as compared to other techniques for patterning of colloidal nanoparticles, the technique demonstrated in the paper is capable to place a single colloidal nanoparticle onto the semiconductor surface with precision of several nanometers, thus allowing growth of a single nanowire at the location of interest, which has not been demonstrated by any technique so far.
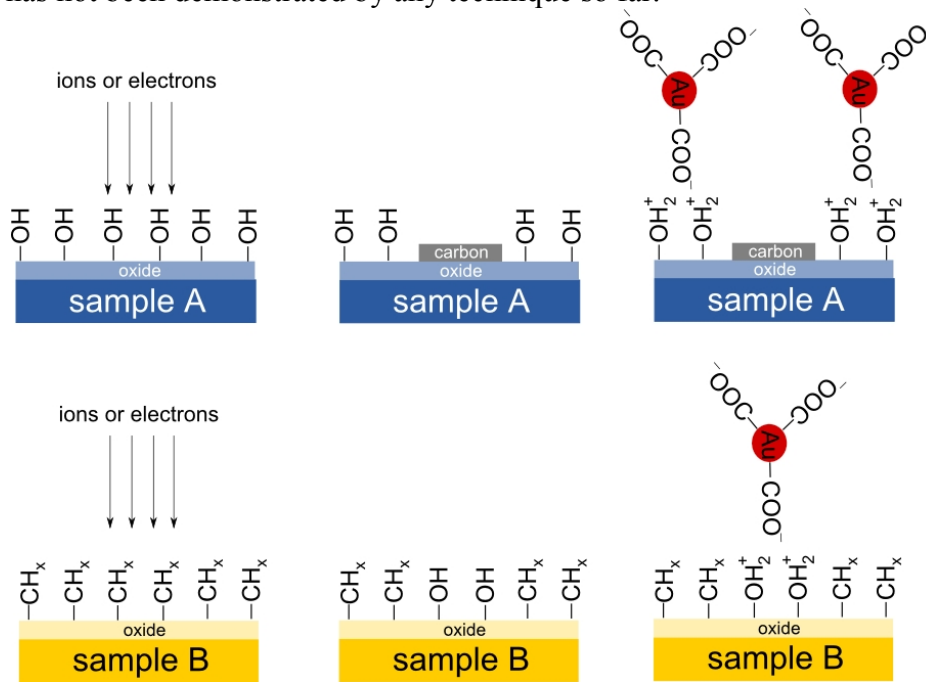
Fig. 8: *A scheme depicting selective deposition of nanoparticles from colloidal solution onto a semiconductor surface. Top: hydroxyl terminated silicon surface with native oxide layer. After a long exposure to a particle beam, amorphous carbon layer is formed. Immersion of such a sample into acidic colloidal solution (citrate-terminated gold nanoparticles) results in selective adsorption of nanoparticles onto unexposed areas only, due to electrostatic interaction of negatively charged $-COO^-$ and positively charged $-OH_2^+$ groups. Bottom: The same surface functionalized by $-CH_3$ exhibits opposite behavior if exposed by low particle fluence. The surface groups are exchanged for hydroxyls and upon immersion in acidic colloidal solution the nanoparticles adhere to the exposed areas only.*

8.2 Commented paper 6, dealing with dopant concentration analysis[6]

Doping of semiconductors is undoubtedly a key process in current semiconductor technology. However, as the dimensions of the relevant devices shrink, new concerns are raised about the prospects of doping and its limitations [57] as well as the quantitative analysis of dopant atoms concentration and their spatial distribution in such a small volume. Naturally, this concerns nanowires as well. The doping of nanowires is usually made by introducing a dopant-containing precursor gas into the vacuum chamber (e.g. phosphine) and the dopants are embedded into the nanowire via VLS process. It is currently understood that dopants are incorporated into the nanowire nonuniformly, as their concentration is the highest close to the nanowire surface. This results from two independent effects [58]: (i) uncatalyzed vapor-solid deposition of dopants onto the nanowires' sidewalls [59] and (ii) preferential incorporation of dopants close to the triple phase boundary, where the liquid-solid interface is faceted and supersaturation the highest (see section 2.3) [60]. A detailed knowledge on dopant atom spatial distributions within a single nanowire was gathered utilizing Atom Probe Tomography (APT), a technique based on Field Ion Microscopy which was developed in 1950s by E. Muller and allowed to "see the atoms" for the first time in history. The technique is microscopic, allowing identification of the atomic positions within a nanowire, while simultaneously providing chemical information (by measuring the time-of-flight of ionized atoms from a sample to a detector). However, this technique suffers from a very troublesome sample preparation, which is even more complicated than e.g. TEM lamella preparation (see next section 8.3). While the spatial distributions of dopant atoms within a nanowire are possible to sample with ATR and TEM, more possibilities exist concerning dopant concentrations. Here, traditional techniques like Secondary Ion Mass Spectroscopy (SIMS) are particularly useful. However, the simplest way to detect dopant concentrations in a nanoscopic sample seems to be a contrast-based detection in an SEM (where p-doped regions appear brighter), which is a focus of Commented paper 6.

In this paper we were looking for an optimum sample preparation procedure and for such observation conditions that maximize the image contrast related to different dopant atom concentrations. Although the exact mechanism of dopant contrast is unknown, it is generally accepted that it has an electronic origin (work-function changes or surface band-bending) and, hence, it is critically dependent on the surface conditions. This is demonstrated by our experiments, where thin surface oxide layer (grown during sample exposure to ambient conditions or plasma cleaning) or carbon contamination (due to repetitive electron beam scanning across the sample) significantly deteriorate the contrast. For the same reasons, the energy of primary electrons (which determines the sampling depth) has to be kept quite low (<1 keV) to effectively increase the contrast.

We have shown that if the surface is carefully treated the dependence of image contrast on dopant concentration is logarithmic, which could be utilized to assess the dopant concentration quantitatively down to 10^{16} cm^{-3}. However, the technique has also several drawbacks: reference is needed (this is usually a substrate of known dopant concentration) and, more importantly, a lot of other effects can affect the contrast formation in secondary electron image, mostly surface topography. The technique was already applied to nanowire samples [61] and represents a low-cost

---

[6] Druckmüllerová, Z.; Kolíbal, M.; Vystavěl, T.; Šikola, T. *Towards site-specific dopant contrast in scanning electron microscopy*, Microsc. & Microanal. 2014, 20, 1312.

alternative to established powerful tools requiring expensive dedicated instrumentation. On top of that, as the dopant contrast in secondary electron images is of electronic origin and not because of Z-contrast, it allows quantification of the *activated* dopants concentration. Note that this is not the case of the above mentioned techniques, which detect the dopant atoms irrespective of their electronic state.

8.3 Commented paper 7, dealing with germanium nanofabrication[7]

The Commented paper 7 deals mostly with the effect of scanning strategy onto the resulting morphology of structures prepared by focused ion beam milling. While majority of the experiments was performed with silicon, we have also investigated the behavior of germanium substrate. We have demonstrated that material swelling due to amorphization of the semiconductor substrate under the influence of an energetic ion beam is enormous in case of germanium. We have found out that to suppress this phenomenon the energy of the ions has to be decreased, which is rationalized by reduced energy transfer to the substrate atoms. Naturally, this finding is important for ion beam patterning of semiconductor substrates. However, it is crucial also for TEM sample preparation.

For TEM inspection, nanowires are usually detached from the substrate by sonication in isopropanol and subsequently drop-cast on a copper mesh. However, if the substrate-nanowire interface is in question, it is necessary to prepare a TEM lamella by focused ion beam. This procedure starts with deposition of a protective platinum layer over a nanowire and as a next step two trenches are milled on both sides of the nanowire by high-energy (30 keV) focused ion beam (see Fig. 9a)). For germanium, this procedure is uneasy due to a large damage done to the substrate (and the nanowire) by the ion beam. Based on the results of Commented paper 7 we have modified it by decreasing the ion beam energy during the initial milling step. The quality of the prepared sample allows for inspection of defects at the substrate-nanowire interface (Fig. 9b)) and even to achieve an atomic resolution (not shown).
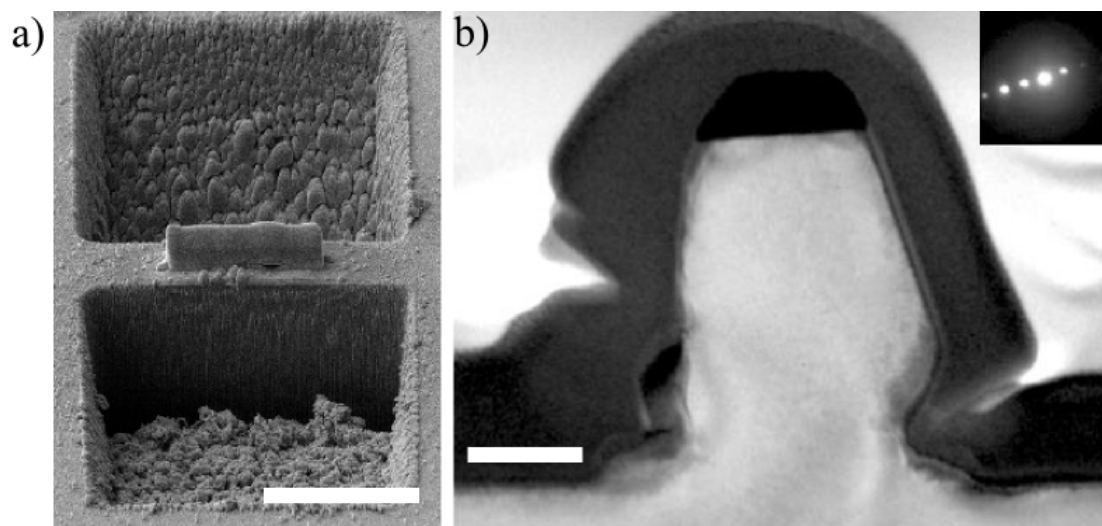
Fig. 9*: a) A double trench milled into a Ge(111) substrate by 30 keV Ga ion beam. A small rectangular object in the middle between trenches is a platinum deposit, protecting the nanowire (not visible) from an ion beam damage. The extreme swelling*

[7] Kolíbal, M.; Matlocha, T.; Vystavěl, T.; Šikola, T. *Low energy focused ion beam milling of silicon and germanium nanostructures*. Nanotechnology 2011, 22, 105304.

and amorphization of the substrate is clearly visible in the image and, hence, additional thinning of the lamella is pointless. Scale bar, 10 μm. Sample preparation by Eva Kolíbalová. b) TEM image of a Ge NW prepared by low energy ion beam milling. No structural defects are visible at the substrate-nanowire interface. The inset shows an electron diffraction pattern, proving that nanowires are crystalline. Scale bar, 200 nm. Sample preparation and imaging by Tomáš Vystavěl.

9. Conclusions and outlook

In this habilitation thesis the contribution of our group to the field of one-dimensional nanostructure growth was presented. Basic concepts of the VLS growth were described, together with the concept of preferential nucleation and the Gibbs-Thompson effect, which hinders the growth of ultra-small nanowires. Next, four papers of our group are attached. It should be additionally remarked here that the main focus of our papers are germanium nanowires (Commented papers 1-3), while the 4th commented paper deals with silicon oxide nanowires. The last section demonstrates other issues related to analysis of nanowire properties and growth, with three papers attached. Our germanium-related research is focused onto the behavior of the collector droplet and its effect on the nanowire morphology and growth direction. Commented paper 4 presents a strikingly different system, where a large amount of nanowires grow from a single large gallium droplet. This system represents an elegant way to circumvent the Gibbs-Thompson effect in an attempt to grow nanowires with extremely small diameters. The main added value of these papers in general is a real-time microscopic observation, possible via development of a heating stage minimizing temperature drifts and a reaction chamber, allowing for observation at high pressures. The experimental observations shown here contribute to the general understanding of the one-dimensional nanowire growth. Indeed, the research is driven by applications, mainly in semiconductor industry and optoelectronics, and there is still a lot of unresolved issues. Here, two of them will be mentioned, as they actually outline my current nanowire-oriented research.

One of such fundamental issues is the incorporation of the collector material into the nanowire and nanowire doping, which are closely related subjects. There are contradictory reports in the literature whether the atoms from the collector droplet can be incorporated into the nanowire or not. The main interest in this particular issue was the complicated utilization of gold-catalyzed nanowires in semiconductor industry, because gold is known to create defect mid-gap states in silicon. Recent studies tend to confirm the presence of collector material inside the NWs [14, 62]. However, together with the intensive research of alternative metal seeds, this finding became technologically important as the collector material can be in principle utilized for doping. This unique approach could reignite the use of liquid metals as metal seeds for nanowire growth. From my point of view, a potentially promising candidate for collector-mediated doping of germanium is antimony, because it exhibits a similar phase diagram to Au-Ge (eutectic point at 592 °C at 15% Ge concentration). The controllable incorporation of collector material into the nanowire is an exciting way to alter also other properties of germanium, e.g. direct band gap formation by addition of tin or inducing magnetic properties by manganese incorporation. I am currently going to focus on nanowire growth utilizing alloyed catalysts, because possibilities of their usage seem endless, as the collector composition could be tuned to achieve desired nanowire properties.

Another important topic is nanowire kinking towards other crystallographic directions. From numerous papers it seems that nanowire orientation can be controlled

by different means, e.g. by growth kinetics (Commented paper 1) or changes in surface chemistry [48, 63]; however, the full understanding of the problem is still missing [64,65]. There are good reasons for the interest in kinking mechanism. Growth of nanowire heterostructures is indispensably accompanied by the change of material supply and, hence, droplet supersaturation, which we have shown to result in nanowire kinking. Indeed, this is considered to be unintentional effect and, hence, is investigated in detail by nanowire growth community. I have just recently started to study the effects of atomic hydrogen on the nanowire growth direction and droplet stability. As the adsorbed atoms and molecules are known to drastically alter the surface free energy, it is reasonable to expect various effects on the nanowire growth (e.g. see eq. (4)) and our recent results with hydrogen confirm all these assumptions. I will direct my research activities towards the use of other adsorbates (sulphur and methyl groups, for example) to achieve a controllable fully three-dimensional growth.

Nanowire research combines physics, material science and chemistry and as such represents an exciting and stimulating playground for many scientists around the world. Although first nanowire-based devices are already commercially available, new functionalities already demonstrated on the laboratory level are even more promising. Nevertheless, there are still many issues and hidden mechanisms that need to be revealed to exploit the full potential of one-dimensional nanostructures and I am convinced that some of these puzzles will be solved in our laboratory.

References

[1] Prokes S. M. and Arnold S. *Stress-driven formation of Si nanowires.* Appl. Phys. Lett. 2005, 86, 193105

[2] Rudolph, D.; Hertenberger, S.; Bolte, S.; Paosangthong, W.; Spirkoska, D.; Döblinger, M.; Bichler, M.; Finley, J. J.; Abstreiter, G.; Koblmüller, G. *Direct observation of a noncatalytic growth regime for GaAs nanowires.* Nano Letters 2011, 11, 3848-3854.

[3] Consonni, V.; Knelangen, M.; Geelhaar, L.; Trampert, A.; Riechert, H. *Nucleation mechanisms of epitaxial GaN nanowires: Origin of their self-induced formation and initial radius.* Phys. Rev. B 2010, 81, 085310.

[4] Bertness, K. A.; Roshko, A.; Mansfield, L. M.; Harvey, T. E.; Sanford, N. A. *Mechanism for spontaneous frowth of GaN nanowires with molecular beam epitaxy.* J. Cryst. Growth 2008, 310, 3154.

[5] Bierman, M. J.; Albert Lau, Y. K.,; Kvit, A.V.; Schmitt, A. L.; Jin, S. *Dislocation-driven nanowire growth and Eshelby twist.* Science 2008, 320, 1060.

[6] Wagner, R. S.; Ellis W. C. *Vapor-liquid-solid mechanism of single crystal growth.* Appl. Phys. Lett. 1964, 4, 89.

[7] Wacaser, B. A.; Dick, K. A.; Johansson, J.; Borgström, M. T.; Deppert, K.; Samuelson, L. *Preferential Interface Nucleation: An Expansion of the VLS Growth Mechanism for Nanowires.* Adv. Mater. 2009, 21, 153.

[8] Jenke, M. G.; Lerose, D.; Niederberger, C.; Michler, J.; Christiansen, S.; Utke, I. *Toward local growth of individual nanowires on three-dimensional microstructures by using a minimally invasive catalyst templating method.* Nano Letters 2011, 11, 4213.

[9] Okamoto, H. and Massalski, T. B. *The Au-Ge system.* Bulletin of Alloy Phase Diagrams 1984, 5, 601.

[10] Sutter, E.; Sutter, P. *Phase Diagram of Nanoscale Alloy Particles Used for Vapor-Liquid-Solid Growth of Semiconductor Nanowires.* Nano Letters 2008, 8, 411.

[11] Gamalski, A. D.; Tersoff, J.; Sharma, R.; Ducati, C.; Hofmann, S. *Formation of metastable liquid catalyst during subeutectic growth of germanium nanowires.* Nano Letters 2010, 10, 2972.

[12] Putnam, M. C.; Filler, M. A.; Kayes, B. M.; Kelzenberg, M. D.; Guan, Y.; Lewis, N. S.; Eiler, J. M.; Atwater, H. A. *Secondary ion mass spectrometry of vapor-liquid-solid grown, Au catalyzed, Si wires.* Nano Letters 2008, 8, 3109.

[13] Allen J. E.; Hemesath, E. R.; Perea, D. E.; Lensch-Falk, J. L.; Li, Z. Y.; Yin, F.; Gass, M. H.; Wang, P.; Bleloch, A. L.; Palmer, R. E.; Lauhon, L. J. *High-resolution detection of Au catalyst atoms in Si nanowires.* Nature Nanotechnology 2008, 3, 168.

[14] Moutanabbir, O.; Isheim, D.; Blumtritt, H.; Senz, S.; Pippel, E.; Seidman, D. N. *Colossal injection of catalyst atoms into silicon nanowires.* Nature 2013, 496, 78.

[15] Koren, E.; Elias, G.; Boag, A.; Hemesath, E. R.; Lauhon, L. J.; Rosenwanks, Y. *Direct measurement of individual deep traps in single silicon nanowires.* Nano Letters 2011, 11, 2499.

[16] Nebol'sin, V. A., Shchechitin A. A. *Critical Parameters of the Vapor–Liquid–Solid Growth of Silicon Whiskers.* Inorg. Mater. 2003, 39, 899.

[17] Zardo, I.; Yu, L.; Conesa-Boj, S.; Estrade, S.;Alet, P. J..; Rössler, J.; Frimmer, M.; Roca I Cabarrocas, P.; Peiró, F.; Arbiol, J.; Morante, J. R.; Fontcuberta i Morral, A. *Gallium assisted plasma enhanced chemical vapor deposition of silicon nanowires.* Nanotechnology 2009, 20, 155602.

[18] Wang, Y.; Schmidt, V.; Senz, S.; Gösele, U. *Epitaxial growth of silicon nanowires using an aluminium catalyst.* Nature Nanotechnology 2006, 1, 186.

[19] Kodambaka, S.; Tersoff, J.; Reuter, M. C.; Ross, F. M. *Germanium nanowire growth below the eutectic temperature.* Science 2007, 316, 729.

[20] Bootsma, G. A. and Gassen, H. J. *A quantitative study on the growth of silicon whiskers from silane and germanium whiskers from germane.* J. Cryst. Growth 1971, 10, 223.

[21] Schmidt, V.; Wittemann, J. V.; Gösele, U. *Growth, thermodynamics and electrical properties of silicon nanowires.* Chem. Rev. 2010, 110, 361.

[22] Olesinski, R. W.; Abbaschian, G. J. *The Ga-Ge system.* Bulletin of Alloy Phase Diagrams 1985, 6, 258.

[23] Butt, M. T. Z. *Study of gold-based alloy phase diagrams.* PhD thesis, The University of West London, 1990.

[24] Wen, C. –Y.; Reuter, M. C.; Tersoff, J.; Stach, E. A.; Ross, F. M. *Structure, growth kinetics, and ledge flow during vapor-solid-solid growth of copper-catalyzed silicon nanowires.* Nano Letters 2010, 10, 514.

[25] Givargizov, E. I. *Fundamental aspects of VLS growth.* J. Cryst. Growth 1975, 31, 20.

[26] Dayeh, S. A.; Picraux, S. T. *Direct observation of nanoscale size effects in Ge semiconductor nanowire growth.* Nano Letters 2010, 10, 4032.

[27] Fröberg, L. E.; Seifert, W.; Johansson, J. *Diameter-dependent growth rate of InAs nanowires.* Phys. Rev. B 2007, 76, 153401.

[28] Gibbs, J. W. *On the equilibrium of heterogenous substances.* Trans. Connect. Acad. Sci. 1878, 16, 343.

[29] De Yoreo, J. J.; Vekilov, P. G. *Principles of Crystal Nucleation and Growth*, Revs. Min. and Geochem. 2003, 54, 57.

[30] Gamalski, A. D., Ducati, C., Hoffmann, S. *Cyclic supersaturation and triple phase boundary dynamics in germanium nanowire growth*. J. Phys. Chem. C 2011, 115, 4413.

[31] Ross, F.M. *Controlling nanowire structures through real time growth studies*. Rep. Prog. Phys. 2010, 73, 114501.

[32] Kim, B. J.; Tersoff, J.; Wen, C. –Y.; Reuter, M. C.; Stach, E. A.; Ross, F. M. *Determination of size effects during the phase transition of a nanoscale Au-Si eutectic*. Phys. Rev. Lett. 2009, 103, 155701.

[33] Kim, B. J.; Tersoff, J.;Kodambaka, S.;Reuter, M. C.; Stach, E. A.; Ross, F. M. *Kinetics of individual nucleation events observed in nanoscale vapor-liquid-solid growth*. Science 2008, 322, 1070.

[34] Wen, C.-Y.; Tersoff, J.; Reuter, M. C.; Stach, E. A.; Ross, F. M. *Step-flow kinetics in nanowire growth*. Phys. Rev. Lett. 2010, 105, 195502.

[35] Schmidt, V.; Senz, S.; Gosele, U. *The shape of epitaxially grown silicon nanowires and the influence of line tension*. Applied Physics A 2005, 80, 445.

[36] Schwarz, K. W.; Tersoff, J. *From droplets to nanowires: dynamics of vapor-liquid-solid growth*. Phys. Rev. Lett. 2009, 102, 206101.

[37] Schwarz, K. W., Tersoff, J. *Elementary Processes in Nanowire Growth*. Nano Letters 2011, 11, 316.

[38] Wu, Y.; Cui, Y.; Huynh, L.; Barrelet, C. J.; Bell, D. C.; Lieber, C. M. *Controlled Growth and Structures of Molecular-Scale Silicon Nanowires*. Nano Letters 2004, 4, 433.

[39] Schmidt, V.; Senz, S.; Gösele, U. *Diameter-dependent growth direction of epitaxial silicon nanowires*. Nano Letters 2005, 5, 931.

[40] Kodambaka, S.; Tersoff, J.; Reuter, M. C.; Ross, F. M. *Diameter-independent kinetics in the vapor-liquid-solid growth of Si nanowires*. Phys. Rev. Lett. 2006, 96, 096105.

[41] Uccelli, E.; Arbiol, J.; Magen, C.; Krogstrup, P.; Russo-Averchi, E.; Heiss, M.; Mugny, G.; Morier-Genoud, F.; Nygard, J.; Morante, J. R.; Fontcuberta i Morral, A.; *Three-dimensional multiple-order twinning of self-catalyzed GaAs nanowires on Si substrates*. Nano Letters 2011, 11, 3827.

[42] Schwarz, K. W.; Tersoff, J.; Kodambaka, S.; Chou, Y. –C.; Ross, F. M. *Geometrical Frustration in Nanowire Growth*. Phys. Rev. Lett. 2011, 107, 265502.

[43] Schwarz, K. W.; Tersoff, J.; Kodambaka, S.; Ross, F. M. *Jumping-catalyst dynamics in nanowire growth*. Phys. Rev. Lett. 2014, 113, 055501.

[44] Fortuna, S. A.; Li, X. *Metal-catalyzed semiconductor nanowires: a review on the control of growth directions*. Semicond. Sci. Technol. 2010, 25, 024005.

[45] Hanrath, T.; Korgel, B. A. *Crystallography and surface faceting of germanium nanowires.* Small 2005, 1, 717.

[46] Ross, F. M., Tersoff, J., Reuter, M. C. *Sawtooth Faceting in Silicon Nanowires.* Phys. Rev. Lett. 2005, 95, 146104.

[47] Stekolnikov, A. A.; Bechstedt, F. *Shape of free and constrained group-IV crystallites: Influence of surface energies.* Phys. Rev. B 2005, 72, 125326.

[48] Sivaram, S. V.; Shin, N.; Chou, L.-W.; Filler, M. A. *Direct observation of transient surface species during Ge nanowire growth and their influence on growth stability.* J. Am. Chem. Soc. 2015, 137, 9861.

[49] Adhikari, H.; Marshall, A. F.; Goldthorpe, I. A.; Chidsey, C. E. D.; McIntyre, P. C. *Metastability of Au-Ge liquid nanocatalysts: Ge vapor-liquid-solid nanowire growth far below the bulk eutectic temperature.* ACS Nano 2007, 1, 415. Also: Kim, B. J.; Wen, C.-Y.; Tersoff, J.; Reuter, M. C.; Stach, E. A.; Ross, F. M. *Growth pathways in ultralow temperature Ge nucleation from Au.* Nano Letters 2012, 12, 5867.

[50] Michael Filler, private communication.

[51] Perea, D. E.; Li, N.; Dickerson, R. M.; Misra, A.; Picraux, S. T. *Controlling heterojunction abruptness in VLS-grown semiconductor nanowires via in situ catalyst alloying.* Nano Letters 2011, 11, 3117.

[52] Sun, X.; Calebotta, G; Yu, B.; Selvaduray, G.; Meyyappan, M. *Synthesis of germanium nanowires on insulator catalyzed by indium and antimony.* J. Vac. Sci. Technol. B 2007, 25, 415. Also Sun, R.; Jacobsson, D.; Chen, I-J.; Nilsson, M.; Thelander, C.; Lehmann, S.; Dick, K. A. *Sn-seeded GaAs nanowires as self-assembled radial p-n junctions.* Nano Letters 2015, 15, 3757.

[53] Pan, Z. W.; Dai, Z. R.; Ma, C.; Wang, Z. L. *Molten gallium as a catalyst for the large-scale growth of highly aligned silica nanowires.* J. Am. Chem. Soc. 2002, 124, 1817.

[54] Kolasinski, K. W. *Catalytic growth of nanowires: vapor-liquid-solid, vapor-solid-solid, solution-liquid-solid and solid-liquid-solid growth.* Curr. Opinion in Solid State and Mat. Sci. 2006, 10, 182.

[55] Chandrasekaran, H.;Sumanasekara, G. U.; Sunkara, M. K. *Rationalization of nanowire synthesis using low-melting point metals.* J. Phys. Chem. B 2006, 110, 18351.

[56] Weick, G.; Woollacott, C.; Barnes, W. L.; Hess, O.; Mariani, E. *Dirac-like plasmons in honeycomb lattices of metallic nanoparticles.* Phys. Rev. Lett. 2013, 110, 106801.

[57] Erwin, S. C.; Zi, L.; Haftel, M. I.; Efros, A. L.; Kennedy, T. A.; Norris, D. J. *Doping semiconductor nanocrystals.* Nature 2005, 436, 91.

[58] Amit, I.; Givan, U.; Connell, J. G.; Paul, D. F.; Hammond, J. S:; Lauhon, L. J.; Rosenwanks, Y. *Spatially resolved correlation of active and total doping concentrations in VLS grown nanowires.* Nano Letters 2013, 13, 2598.

[59] Perea, D. E.; Hemesath, E. R.; Schwalbach, E. J.; Lensch-Falk, J. L.; Voorhees, P. W.; Lauhon, L. J. *Direct measurement of dopant distribution in an individual vapour-liquid-solid nanowire.* Nature Nanotechnol. 2009, 4, 315.

[60] Connell, J. G.; Yoon, K., Perea, D. E.; Schwalbach, E. J.; Voorhees, P. W.; Lauhon, L. J. *Identification of an intrinsic source of doping inhomogeneity in vapor-liquid-solid-grown nanowires.* Nano Letters 2013, 13, 199.

[61] Tchoulfian, P.; Donatini, F.; Levy, F.; Dussaigne, A.; Ferret, P.; Pernot, J. *Direct imaging of p-n junction in core-shell GaN wires.* Nano Letters 2014, 14, 3491.

[62] Chen, W.; Yu, L.; Misra, S.; Fan, Z.; Pareige, P.; Patriarche, G.; Bouchole, S.; Roca i Cabarrocas, P. *Incorporation and redistribution of impurities into silicon nanowires during metal-particle-assisted growth.* Nat. Comms. 2014, 5, 1.

[63] Kodambaka, S.; Hannon, J. B.; Tromp, R. M.; Ross, F. M. *Control of Si nanowire growth by oxygen.* Nano Letters 2006, 6, 1292.

[64] Hocevar, M.; Immink, G.; Verheijen, M.; Akopian, N.; Zwiller, V.; Kouwenhoven, L,; Bakkers, E. *Growth and optical properties of axial hybrid III–V/silicon nanowires.* Nat. Comms. 2012, 3, 1266.

[65] Hillerich, K.; Dick, K.A.; Wen, C.-Y.; Reuter, M. C.; Kodambaka, S.; Ross, F. M. *Strategies To Control Morphology in Hybrid Group III−V/Group IV Heterostructure Nanowires.* Nano Letters 2013, 13, 903.